



Novel Sodium Channel Inhibitor From Leeches

Gan Wang^{1†}, Chengbo Long^{1†}, Weihui Liu^{1†}, Cheng Xu¹, Min Zhang^{1,2}, Qiong Li³, Qiumin Lu^{1,4}, Ping Meng¹, Dongsheng Li¹, Mingqiang Rong^{1,4}, Zhaohui Sun^{5*}, Xiaodong Luo^{3*} and Ren Lai^{1,6*}

¹ Key Laboratory of Bioactive Peptides of Yunnan Province/Key Laboratory of Animal Models and Human Disease Mechanisms of Chinese Academy of Sciences, Kunming Institute of Zoology, Kunming, China, ² Graduate School of University of Chinese Academy of Sciences, Beijing, China, ³ State Key Laboratory of Phytochemistry and Plant Resources in West China, Kunming Institute of Botany, Chinese Academy of Sciences, Kunming, China, ⁴ Sino-African Joint Research Center, Chinese Academy of Sciences, Wuhan, China, ⁵ Department of Clinical Laboratory, Guangzhou General Hospital of Guangzhou Military Command of PLA, Guangzhou, China, ⁶ Life Sciences College of Nanjing Agricultural University, Nanjing, China

OPEN ACCESS

Edited by:

Yuri N. Utkin,
Institute of Bioorganic Chemistry
(RAS), Russia

Reviewed by:

Vladimir Yarov-Yarovoy,
University of California, Davis,
United States
Roope Mannikko,
University College London,
United Kingdom

*Correspondence:

Ren Lai
rlai@mail.kiz.ac.cn
Xiaodong Luo
xdluo@mail.kib.ac.cn
Zhaohui Sun
zhaohui3@126.com

† These authors have contributed
equally to this work.

Specialty section:

This article was submitted to
Pharmacology of Ion Channels
and Channelopathies,
a section of the journal
Frontiers in Pharmacology

Received: 21 November 2017

Accepted: 19 February 2018

Published: 06 March 2018

Citation:

Wang G, Long C, Liu W, Xu C,
Zhang M, Li Q, Lu Q, Meng P, Li D,
Rong M, Sun Z, Luo X and Lai R
(2018) Novel Sodium Channel
Inhibitor From Leeches.
Front. Pharmacol. 9:186.
doi: 10.3389/fphar.2018.00186

Considering blood-sucking habits of leeches from surviving strategy of view, it can be hypothesized that leech saliva has analgesia or anesthesia functions for leeches to stay undetected by the host. However, no specific substance with analgesic function has been reported from leech saliva although clinical applications strongly indicated that leech therapy produces a strong and long lasting pain-reducing effect. Herein, a novel family of small peptides (HSTXs) including 11 members which show low similarity with known peptides was identified from salivary glands of the leech *Haemadipsa sylvestris*. A typical HSTX is composed of 22–25 amino acid residues including four half-cysteines, forming two intra-molecular disulfide bridges, and an amidated C-terminus. HSTX-I exerts significant analgesic function by specifically inhibiting voltage-gated sodium (Na_v) channels (Na_v1.8 and Na_v1.9) which contribute to action potential electrogenesis in neurons and potential targets to develop analgesics. This study reveals that sodium channel inhibitors are analgesic substances in the leech. HSTXs are excellent candidates or templates for development of analgesics.

Keywords: leech therapy, blood-sucking, sodium channel, pain, analgesia

INTRODUCTION

As specific bloodsucking ectoparasites, leeches have to penetrate hosts' body surface and suppress the reactions of hosts to injuries, such as swelling, pain, and inflammation to remain undetected and successfully get blood meal, suggesting that anesthetic agents may delivered during the blood-sucking process. Furthermore, they have to overcome hemostatic and vasoconstriction reactions in hosts to ensure a steady and sustained blood flow to the feeding site. Leeches inject saliva into hosts to counteract the reactions of hosts.

With many clinically challenges, pain affects millions of individuals worldwide and remains poorly understood. VGSCs (voltage-gated sodium channels) are essential for pain perception because they play a critical role in the generation and propagation of action potentials in excitable cells, including neurons, muscle cells, and cardiomyocytes. Nine subtypes (Na_v1.1–1.9) of VGSCs have been identified in mammals. VGSCs have been broadly classified as TTX-S (TTX-sensitive)

and TTX-R (TTX-resistant) by their sensitivities to tetrodotoxin (TTX). The majority of DRG (dorsal root ganglion) neurons express at least six Nav subtypes (Cummins et al., 1999; Waxman et al., 1999): Nav1.1, Nav1.6, Nav1.7, Nav1.8, Nav1.9, and Nav (Dib-Hajj et al., 1998). The TTX-S Nav current produced by Nav1.1, Nav1.6 and Nav1.7 is fast-inactive. Whereas, Nav1.8 and Nav1.9 produce the slow-inactivating TTX-R current (Akopian et al., 1996).

Different sodium channel subtypes have specific distributions and functions. Sodium channel Nav1.8 is mainly expressed in peripheral neurons, in particular within retinal amacrine and ganglion cells (O'Brien et al., 2008), small and medium-sized DRG neurons, and nociceptive afferent fibers (Benn et al., 2001; Shields et al., 2012); Nav1.9 is expressed more widely. It is found in the hippocampus, cortex (Blum et al., 2002), photoreceptors and Müller glia, small diameter DRG, trigeminal ganglia, and the intrinsic sensory neurons of the gut (Fang et al., 2002; Rugiero et al., 2003; Padilla et al., 2007).

Compared with other TTX-S channels, Nav1.8 is known to produce a slow-inactivating TTX-R current and is characterized by significantly depolarized activation and inactivation. Nav1.9 exhibits unique biophysical properties that include a hyperpolarized voltage-dependent activation and inactivation curves that overlap to produce a large 'window current' and very slow activation and inactivation kinetics (Dib-Hajj et al., 2002). Studies in knockout animals have clearly established a role of Nav1.8 in pain (Akopian et al., 1996; Zimmermann et al., 2007). Furthermore, gain-of-function mutations of Nav1.8 have been found in human subjects with painful neuropathies. These mutations in Nav1.8 channel markedly alter the excitability of DRG neurons (Faber et al., 2012; Huang et al., 2013; Han et al., 2014). Similarly, several monogenic human pain disorders are linked to altered Nav1.9 channel function. For example, some mutations in SCN11A (Nav1.9) resulted in a gain of function at the channel level and were associated with increased pain (Zhang et al., 2013; Huang et al., 2014, 2017), whereas in other study, a mutation (L811P) at the Nav1.9 channel resulted in an inability to experience pain (Leipold et al., 2013). In addition, studies using prostaglandin E2, protein kinase C, intracellular GTP γ S (hydrolysis-resistant GTP analog), or G proteins have demonstrated a link between inflammatory pathways and Nav1.9 channel (Baker et al., 2003; Rush and Waxman, 2004; Baker, 2005; Ostman et al., 2008; Ritter et al., 2009). Nav1.9 is important for the perception of pain in response to cold. Cold pain sensation was greatly reduced in neurons from Nav1.9 knockout mice (Leipold et al., 2015; Lolignier et al., 2015). These observations indicate that Nav1.8/9 represents a high-valued target for development of analgesics.

Blood-sucking leeches have been used for medical purposes in humans for more than 2000 years. Leeches have been approved as medicinal materials or medical device in many countries (Hyson, 2005). As a traditional anti-thrombosis medicinal material, leeches have been used in China for over 1000 years. The FDA has approved leeches as a medical device for plastic and reconstructive surgery in July 2004 (Rados, 2004). Recently, leech therapy has been approved as legal therapeutic intervention in Europe. Especially, extensive attention has been

paid for medicinal leech therapy in pain syndromes, such as osteoarthritis, epicondylitis, vertebrogenic pain syndromes/lower back pain, hematoma/swelling/edema/contusion/distortion, varicose veins/leg ulcer/phlebitis/thrombophlebitis, and cancer pain (Koeppen et al., 2014). Analgesic effect of leech therapy has been approved in many clinic trials. The analgesic effect from leech therapy is rapid, effective, and long-lasting in many conditions (Singh, 2010). However, no specific substance with analgesic function has been reported from leech yet. In this study, we identified a novel group of peptides targeting Nav1.8 and Nav1.9 to produce analgesic effect for the first time.

MATERIALS AND METHODS

Collection of Saliva Sample From *H. sylvestris*

Haemadipsa sylvestris (total weight 500 g) was collected from jungles in Yunnan, China. Saliva sample was collected as described below. Living leeches were frozen quickly in liquid nitrogen. Leech saliva located in the subcutaneous of pharynx was separated, collected and triturated by grinder (Joyoung, China) at low temperature. Triturated saliva sample was dissolved in deionized water, and immediately centrifuged to remove debris. The supernatant [crude extract of saliva (CES)] was lyophilized and kept at -20°C till use. All of the experimental protocols using animals were approved by the Animal Care and Use Committee at Kunming Institute of Zoology, Chinese Academy of Sciences (SYDW-2013018).

Peptide Purification

The CES was applied to a Sephadex G-50 gel filtration column (GE Healthcare, 20–100 μm , 2.6 cm \times 100 cm) which was equilibrated with Tris-HCl buffer (50 mM Tris-HCl, pH 8.9). Sample fractionation was performed by eluting the column using Tris-HCl buffer. Each eluted fraction with a volume of 3.0 ml was collected every 10 min and the absorbance of the eluate was measured at 215 and 280 nm. The effects of eluted fractions (desalted) on VGSCs were assayed using whole-cell patch clamp techniques as described below. The fractions containing VGSCs-inhibiting activity were pooled, lyophilized, and resuspended in 10 ml of the Tris-HCl buffer. The fractions were further purified by using RP-HPLC with C18 column (SunFireTM Prep C18, 5 μm , 250 mm \times 10 mm, Waters) by using acetonitrile containing 0.1% trifluoroacetic acid (TFA) as elution solvent. The absorbance at 215 and 280 nm was monitored by UV detector (Waters 2489).

Determination of Amino Acid Sequence

Edman degradation was used to analyze the amino sequence of purified peptides by pulsed liquid-phase sequencer (Applied Biosystems, model 491). Molecular weight was determined by MALDI-TOF-MS (Matrix-assisted laser desorption ionization time-of-flight mass spectrometry, autoflexTM speed, Bruker) by using positive reflector mode and reported as the monoisotopic $[M + H]^+$ ions, with $\pm 0.001\%$ accuracy of mass determinations.

Construction and Screening of *H. sylvestris* Salivary Gland cDNA Library

Total RNA was extracted using TRIzol Reagent (Invitrogen, United States) from salivary gland (100 mg) of *H. sylvestris* according to our previous methods (An et al., 2013). An Oligotex mRNA Mini kit (Qiagen, Duesseldorf, Germany) was used to extract mRNA. cDNA library was constructed by using a Creator SMARTTM cDNA Library Construction Kit (Clontech, Palo Alto, CA, United States) following manufacturer's instructions, and finally a library of about 2×10^6 independent colonies was produced.

Primers HS1 (5'-GGCAATATTCAAGTCGAAGCTTGC-3') designed according to the homologous sequences determined by transcriptome sequencing, and CDS III (5'-ATTCTAGAGG CCGAGGCGGCCGACATG-3') were used for 3' end DNA amplification. Primers HS2 (5'-GAAACATTTTAATTTT TAGA GGTTCATCC-3') designed according to transcriptome data, and CDSIII were used for 5' end DNA amplification. The PCRs were performed by using Advantage polymerase (Clontech, Palo Alto, CA, United States) as follows: 5 min at 95°C followed by 35 cycles of 10 s at 95°C, 30 s at 50°C, 40 s at 72°C, and last 10 min at 72°C. The PCR products were purified by DNA Gel Extraction Kit (Tiangen, China) and ligated into pMD19-T vector (TaKaRa Biotechnology Dalian, Co., Ltd., China) following manufacturer's instructions. DNA sequencing was performed on an Applied Biosystems DNA sequencer (ABI PRISM377).

Intra-molecular Disulfide Bridge Analysis

After incubation in 6 M guanidine solution (pH 3.0) at 37°C for 30 min, native peptide (3 mg) was partially reduced with Tris (2-carboxyethyl) phosphine hydrochloride (0.1 M) at 37°C for 40 min in 0.1 M citrate buffer solution (pH 3.0). The products were purified and lyophilized. The reduced half-cysteines in the peptide were alkylated with 0.5 M iodoacetamide in 0.5 M *N*-methyl morpholine solution (pH 8.3) at 25°C for 30 s. Amino acid sequence of reduced peptide was analyzed by Edman degradation (Wu et al., 1996).

Structure Prediction and Modeling

The structure of HSTX-I was modeled (Supplementary Data Sheet 2) by homology modeling using 3BT4 (PDB ID) as a template. The suitable template for modeling was selected by BLAST result (Supplementary Figure 6) and disulfide bond assignment (Supplementary Figure 2). After suitable template is selected, the PDB file is parsed to extract its sequence. The amino acids of the template are replaced with that of HSTX-I to achieve template sequence alignment. Minimization (QM-MM) protocol was used to minimize the energy of HSTX-I sidechains through geometry optimization using the hybrid delocalized internal coordinate (HDLC) optimizer. The QM region of atoms is treated by a quantum calculation using the DMol³ server and the rest MM is handled by the CHARMM forcefield.

The structure was predicted and modeled using the Discovery Studio (3.1, BIOVIA, San Diego, CA, United States) software and following the data from Edman degradation.

Tissue Distribution of the Analgesic Peptide by qPCR

RNA was extracted from head, body, and tail of *H. sylvestris*, respectively. The expression pattern analyzed by qPCR was repeated three times. HSTX-I and GAPDH primers were designed using IDT Primerquest tools¹ as listed in Supplementary Table 1. SYBR Green PCR kit (Applied Biosystems) was used to perform qPCR. The qPCR procedures were as follows: 5 min of denaturation at 95°C, followed by 40 cycles of amplification with 5 s of denaturation at 94°C, 20 s of annealing according to the melting temperatures provided in Supplementary Table 1 and 15 s of extension at 72°C. The fluorescence data were collected at the end of each cycle. After a final extension at 72°C for 10 min, the specificity of the amplified product was evaluated by melting curve.

Voltage-Clamp and Current-Clamp Recordings

Animal studies followed a protocol (SYDW-2013018) approved by the Animal Care and Use Committee at Kunming Institute of Zoology, Chinese Academy of Sciences. For patch clamp recording, DRG neurons were isolated, as previously reported (Yang et al., 2013). Briefly, rat DRG neurons were harvested and incubated at 37°C for acute dissociation in enzymatic solution [DMEM medium (Corning, NY, United States) with 0.3% collagenase (Sigma, St. Louis, MO, United States) and 0.7% trypsin (Sigma, St. Louis, MO, United States)]. After 20 min, the enzymatic solution was replaced by DMEM complete growth medium with 0.3% trypsin inhibitor (Sigma, St. Louis, MO, United States) and maintained in short-term primary culture. All cells were used within 12 h of isolation.

Ca²⁺, K⁺, and Na⁺ currents were recorded from cells using the whole-cell patch clamp technique performed as previously described (Intlekofer et al., 2013; Leipold et al., 2015; Lolignier et al., 2015; Xu et al., 2015). The P/4 protocol was used to subtract linear capacitive and leakage currents. For sodium channel current recordings on DRG neurons, the bath solution contained the following (in mM): 30 NaCl, 25 D-glucose, 1 MgCl₂, 1.8 CaCl₂, 90 TEA-Cl, 5 CsCl, and 5 HEPES at pH 7.4; the pipettes internal solution contained (in mM): 135 CsF, 10 NaCl, and 5 HEPES at pH 7.4. Adding 300 nM TTX (tetrodotoxin) and neurons diameter (<25 μm) were used for discriminating TTX-R from TTX-S Na_v channels. Cells were activated by a 100-ms step depolarization to -10 mV from a holding potential of -80 mV for Na_v currents. For potassium channel, the external solution was (in mM): 130 NaCl, 5 KOH, 12 D-glucose, 2 CaCl₂, 2 MgCl₂, and 10 HEPES, pH 7.2; pipettes were filled with a solution containing (in mM): 120 KF, 20 NMDG (*N*-methyl-D-glucamine), 11 EGTA, 2 Na-ATP, 0.5 GTP, and 10 HEPES, pH adjusted to 7.2 with KOH. Cells were evoked by a 500-ms depolarizing potential of +10 mV from a holding potential of -80 mV to record K_v currents. For calcium current recording, the pipette internal solution contained the following (in mM):

¹<http://www.idtdna.com/Primerquest/Home/Index>

110 CsCl, 5 MgCl₂, 10 EGTA, 25 HEPES, and 2 Mg-ATP, pH adjusted to 7.2 with CsOH; the bath solution contained the following (in mM): 125 TEA-Cl, 10 BaCl₂, 5 HEPES, 5 D-glucose, pH adjusted to 7.3 with CsOH. Cells were activated by a 150-ms step depolarization to +10 mV from a holding potential of -90 mV for Ca_V currents. ~1 μM TTX was added in potassium and calcium bath solution to block Na_V current. For Na_V1.8 channel voltage-clamp recording, DRG neurons (diameter < 25 μm with 300 nM TTX) were held at -70 mV to inactivate Na_V1.9 channels. Furthermore, neurons with potential contamination of Na_V1.9 current were excluded. For Na_V1.9 channels voltage-clamp recording, Na_V1.8-null mouse DRG neurons (diameter < 20 μm with 300 nM TTX) were activated by a 100-ms step depolarization to -40 mV from a holding potential of -110 mV for Na_V1.9 currents. The bath and pipettes solution for Na_V1.8 and Na_V1.9 contained the following (in mM): 150 NaCl, 2 KCl, 5 D-glucose, 1 MgCl₂, 1.5 CaCl₂, and 10 HEPES at pH 7.3; the pipettes internal solution contained (in mM): 105 CsF, 35 NaCl, 10 HEPES, 10 MgCl₂, and 10 EGTA at pH 7.3.

Concentration-response curves were fitted using the following Variable slope model: $Y = \text{Bottom} + (\text{Top} - \text{Bottom}) / (1 + 10^{-(\text{LogIC}_{50} - X) * \text{HillSlope}})$ where HillSlope is the steepness of the family of curves, Top and Bottom are the fraction of current resistant to inhibition at low toxin concentration and high toxin concentration, respectively. For current-voltage (I-V) relationships, cells were held at -70 mV (-110 mV for Na_V1.9 channels) and depolarized to potentials from -80 mV (-100 mV for Na_V1.9 channels) to +40 mV in 5 mV increments for 100 ms, and peak currents were recorded. Conductance-voltage (G-V) relationships were determined from peak current (I) versus voltage relationships as $G = I / (V - V_{\text{rev}})$, where V was the test potential, and V_{rev} was the extrapolated reversal potential. Steady-state fast inactivation was achieved with a series of 500-ms prepulses -100 mV (-120 mV for Na_V1.9) to +10 mV in 10 mV increments, and the remaining non-inactivated channels were activated by a 40-ms step depolarization to 0 mV (-40 mV for Na_V1.9). Steady-state inactivation curves were fitted using the Boltzmann equation. The patch pipettes with DC resistances of 2-3 M were fabricated from borosilicate glass tubing (VWR micropipettes, 100 mL, VWR, Radnor, PA, United States) using a two-stage vertical microelectrode puller (PC-10, Narishige, Tokyo, Japan) and fire-polished by a heater (Narishige, Tokyo, Japan). Recordings were sampled at a rate of 50 kHz, and filtered at 3 kHz.

Before proceeding to current-clamp recordings, the same amplifier with the same configurations as voltage-clamp recordings was used. Pipette solution and bath solution was the same as previously described. The voltage threshold was determined by the first action potential elicited by a series of 1000 ms depolarizing current injections that increased in 50-pA increments. Cells with unstable (>10% variation) resting membrane and action potential overshoot of <40 mV were excluded for data collection.

All data recordings were performed at room temperature using an Axon Multiclamp 700B amplifier (Molecular Devices, Silicon Valley, CA, United States).

Anti-nociceptive Test

To evaluate anti-nociceptive function of samples on mice (female, 18-22 g), several animal models including formalin-induced paw licking, abdominal writhing induced by acetic acid, and hot plate test were used according to previous methods (Yam et al., 2008). Morphine and saline were used as positive and negative control, respectively.

In formalin-induced paw licking model, mice were injected intraperitoneally with test sample dissolved in 100 μl of saline. Thirty minutes later, animals were injected with 20 μl of 1% (vol/vol) formalin at the subcutaneous tissue on plantar surface of right hind paw. Mice were then placed individually into open polyvinyl cages (20 cm × 40 cm × 15 cm). Times of licking the injected paw were recorded by digital video camera during phase I (0-5 min post-injection) and II (15-30 min post-injection).

In the model of abdominal writhing induced by acetic acid, after 30 min of intraperitoneal injection of test sample in one side of abdomen of mice, 100 μl of 1.5% (vol/vol) acetic acid was injected into the other side of abdomen. Mice were placed into open polyvinyl cages (20 cm × 40 cm × 15 cm) immediately, and nociceptive behaviors were counted cumulatively over a period of 30 min.

For hot plate test, mice (female) were placed on a hot plate (ZH-Z organ measurement system, China) with temperature maintained at 55 ± 0.5°C. The response time between placement of the mice on the plate and licking the paws or jumping was recorded as latency (in seconds). The latency was recorded at 0, 30, 60, 90, and 180 min after the intraperitoneal administration of test sample dissolved in 0.9% saline (Yam et al., 2008).

Data Analysis

Electrophysiological data were analyzed using program Clampfit 10.0 (Molecular Devices) and GraphPad Prism 6. Statistical significance was determined by paired Student's *t*-tests or ANOVA. Other experimental results are expressed as means ± SEM. **P* < 0.05 and ***P* < 0.01 are significantly different compared with the control.

Ethics and Biosecurity Statement

All of the experimental protocols using animals were approved by the Animal Care and Use Committee at Kunming Institute of Zoology, Chinese Academy of Sciences (SYDW-2013018). All the researches involving biohazards, biological select agents, toxins, restricted reagents and venom were approved by the Biosafety Committee of Kunming Institute of Zoology, Chinese Academy of Sciences (KZR-2015047).

RESULTS

Purification of Peptide Possessed Activity to Inhibit VGSCs (Voltage-Gated Sodium Channels)

As illustrated in Supplementary Figure 1A, the extracts of the leech salivary glands were divided into six fractions by Sephadex G-50 gel filtration. Fraction III was found to

inhibit TTX-R (tetrodotoxin-resistant) sodium channel currents and was purified further by a C₁₈ RP-HPLC (reverse-phase high performance liquid chromatography) (Supplementary Figure 1B). A peptide named HSTX-I, which contained activity to inhibit TTX-R sodium channel currents was purified.

Amino Acid Sequence of HSTX-I

The complete amino sequence (ACKEYWECGALFCIEGI CVPMI) of HSTX-I was determined by Automated Edman Degradation. The cDNA sequence encoding the precursor of HSTX-I was cloned from the cDNA library of *H. sylvestris* salivary gland (Figure 1A). The precursor is composed of 49 AA (amino acid) residues including a predicted 25-AA signal peptide, a mature HSTX-I and a glycine at the C-terminal, which provides a -NH₂ for C-terminal amidation like other neuropeptides or antimicrobial peptides (Hosseini et al., 2013; Dennison et al., 2015).

Ten homologous sequences of HSTX-I were also cloned from the cDNA library (Figure 1B). All of them share highly conserved cysteine motifs and signal sequence. BLAST search did not find any similarity to other known peptides or proteins, indicating these peptides are a novel peptide family. Eleven members of this peptide family are found in the cDNA library of the leech salivary glands, which confirms the diversity of the peptide family in this species.

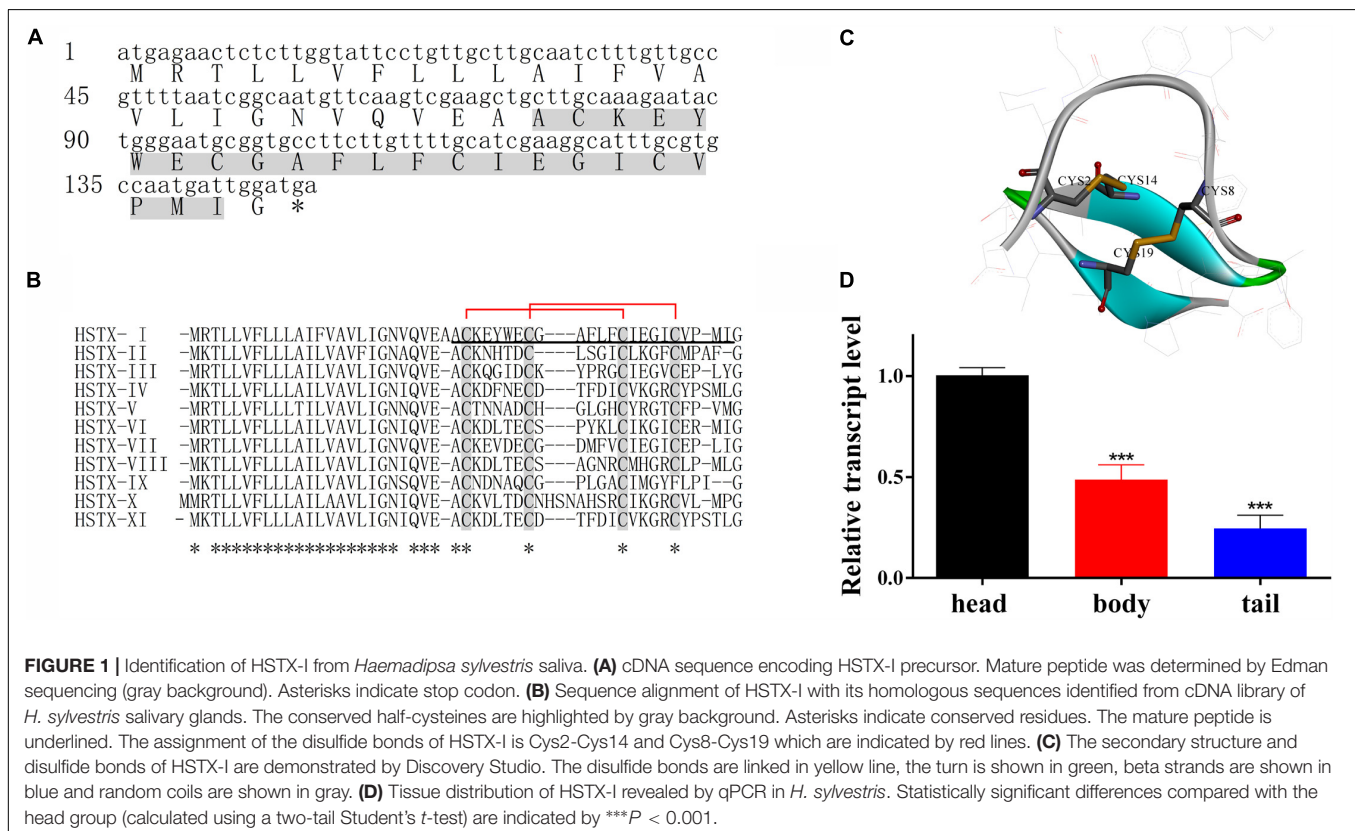
The mature peptide contains four cysteines, which form two intra-molecular disulfide bonds, Cys2-Cys14

and Cys8-Cys19 (Figures 1B,C also see Supplementary Figure 2A). Carboxypeptidase Y treatment did not release the C-terminal amino acid residue, indicating that the C-terminal residue in HSTX-I is amidated. MALDI-TOF mass spectrometry (Supplementary Figure 2B) analysis gave an observed molecular mass of 2621.14 Da which is identical with the calculated molecular mass (2621.17 Da) of HSTX-I with two intra-molecular disulfide bridges and an amidated C-terminus.

The distribution of HSTX-I in leech was evaluated by qPCR (real-time quantitative PCR). The results showed that the expression level of HSTX-I in the head of leech was 2–3 times higher than those in body and tail (Figure 1D).

Effects of HSTX-I on Nav1.8/1.9 Channels

Because HSTX-I showed inhibitory effects on TTX-R sodium channels (see Supplementary Figure 4) including Nav1.8 and Nav1.9, effects of HSTX-I on rNav1.8 (rat Nav1.8) and mNav1.9 (mouse Nav1.9) were investigated. As illustrated in Figure 2, HSTX-I reduced Nav1.8/1.9 currents with IC₅₀ ~2.44 ± 1.42 (Figure 2C) and 3.30 ± 2.48 (Figure 2D) μM, respectively. HSTX-I (3 μM) had no effect on G-V relationship and steady-state inactivation of rNav1.8 (Figure 2E) channels. HSTX-I (3 μM) had no effect on steady-state inactivation of mNav1.9 channels. In contrast, HSTX-I (3 μM) shifted steady-state activation to hyperpolarizability of ~5 mV on mNav1.9 (Figure 2F) channels.



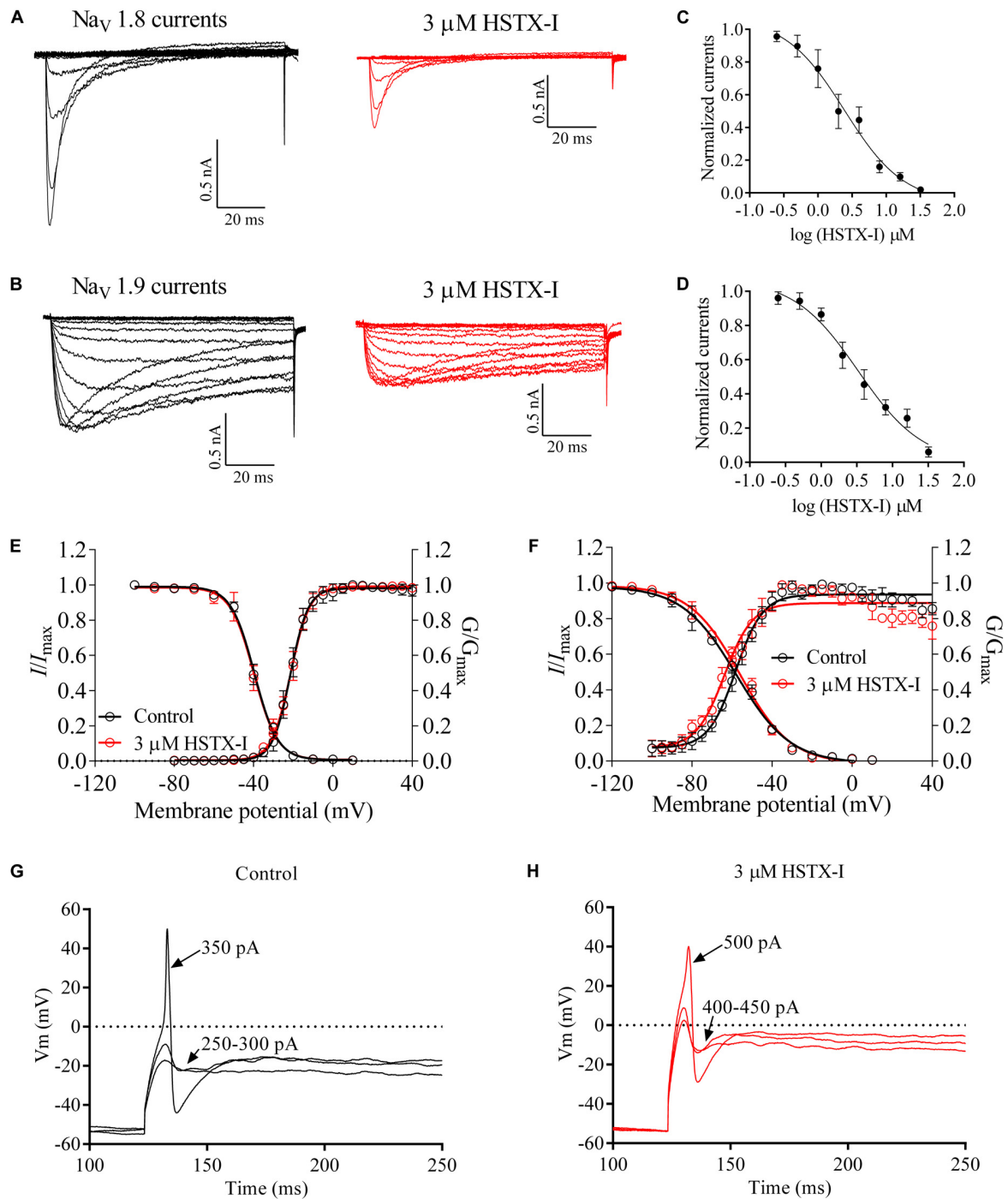
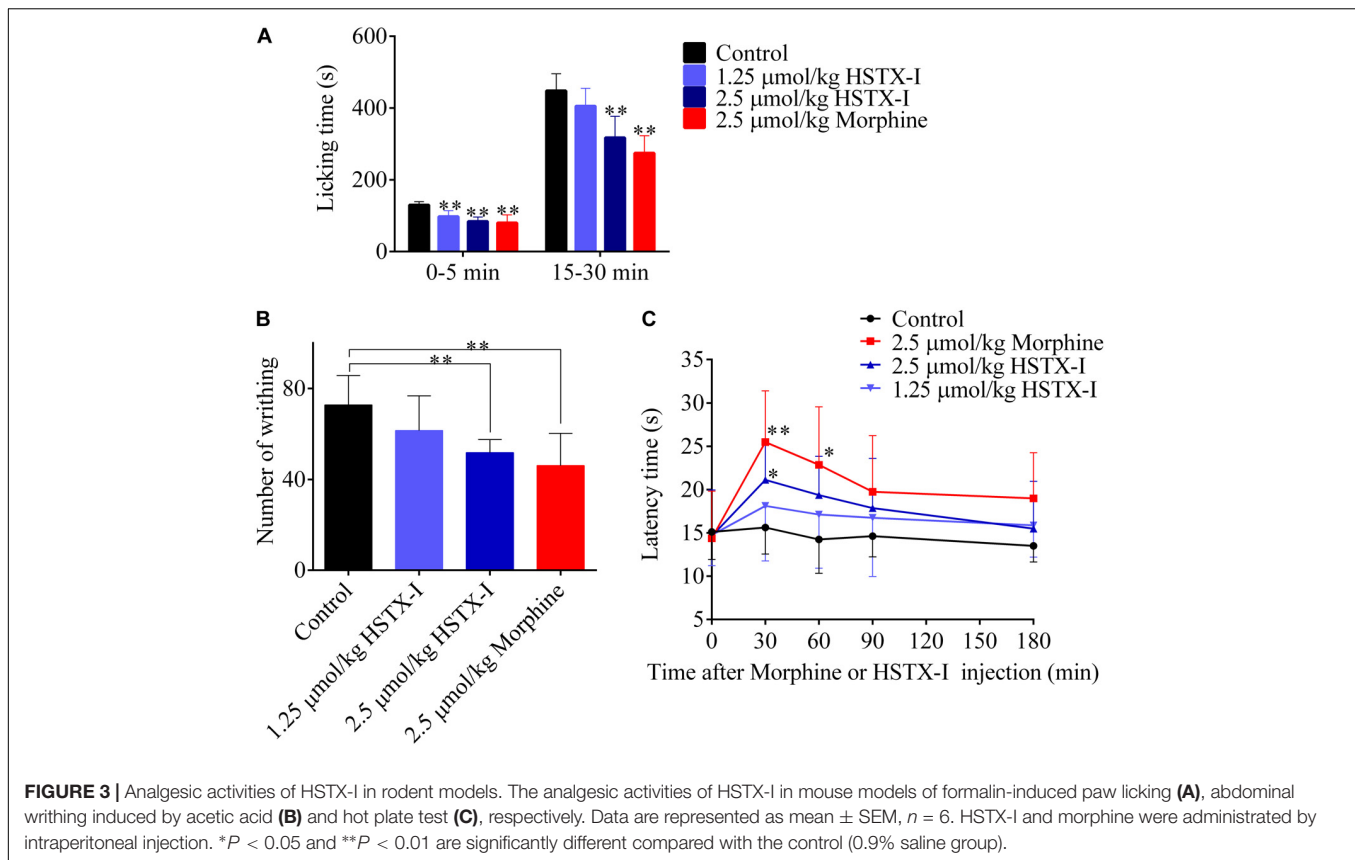


FIGURE 2 | HSTX-I inhibited $\text{Na}_V 1.8/1.9$ channels (also see Supplementary Figure 5). **(A)** Representative current traces of $\text{rNa}_V 1.8$ recorded from the rat small DRG neurons ($< 25 \mu\text{m}$) with 300 nM TTX at holding voltage of -70 mV. **(B)** Representative current traces of $\text{mNa}_V 1.9$, recorded from the $\text{Na}_V 1.8$ -null mouse small DRG neurons (diameter $< 25 \mu\text{m}$ with 300 nM TTX) at holding potential of -110 mV. Control currents are shown in black and the inhibition of $\text{rNa}_V 1.8$ **(A)** and $\text{mNa}_V 1.9$ **(B)** by the indicated concentrations of HSTX-I are shown in red. **(C)** Concentration-response curves for the inhibition of $\text{rNa}_V 1.8$ by HSTX-I. Cells were activated by a 100-ms step depolarization to -10 mV from a holding potential of -70 mV for the IC_{50} of HSTX-I on $\text{rNa}_V 1.8$ channel. **(D)** Concentration-response curves for the inhibition of $\text{mNa}_V 1.9$ by HSTX-I. Cells were activated by a 100-ms step depolarization to -40 mV from a holding potential of -110 mV for the IC_{50} of HSTX-I on $\text{mNa}_V 1.9$ channel. Data are represented as mean \pm SEM. **(E)** Effect of $3 \mu\text{M}$ HSTX-I on the conductance-voltage (G - V) relationship (right) and voltage dependence of steady-state inactivation (left) of $\text{rNa}_V 1.8$ channels. **(F)** HSTX-I ($3 \mu\text{M}$) shifted the G - V relationship of $\text{mNa}_V 1.9$ approximately 5 mV in a negative direction, but it did not induce a shift in steady-state inactivation. **(G)** Responses of a small DRG neuron to the sub-threshold (250–300 pA) and the threshold depolarizing current injections (350 pA). **(H)** Responses of a small DRG neuron treated with $3 \mu\text{M}$ HSTX-I to the sub-threshold (400–450 pA) and the threshold depolarizing current injections (500 pA). Arrows with numbers indicate the current amplitudes used to elicit the responses.



$\text{Nav}_{1.9}$ acts as a threshold channel that regulates excitability of DRG neurons to induce pain. Threshold depolarizing currents of small DRG neurons before and after application of HSTX-I ($3 \mu\text{M}$) were compared as illustrated in **Figures 2G,H**. Average current threshold of controls was $341.7 \pm 15.37 \text{ pA}$ ($n = 6$). After treatment with $3 \mu\text{M}$ HSTX-I, the current threshold was increased to $491.7 \pm 27.13 \text{ pA}$ ($n = 6$) which was significantly larger than that in the control ($P = 0.0007$). **Figure 2G** shows a small DRG neuron responding to subthreshold current injections ($250\text{--}300 \text{ pA}$) and the threshold depolarizing current injections (350 pA) with graded membrane potential depolarizations before application of HSTX-I. After application of HSTX-I ($3 \mu\text{M}$), subthreshold current injections and threshold depolarizing current injections rose to $400\text{--}450$ and 500 pA , respectively (**Figure 2H**).

Analgesic Functions of HSTX-I in Rodent Models

$\text{Nav}_{1.8/1.9}$ are preferentially expressed in nociceptors and have been showed to have a major role in pain (Swanwick et al., 2010; Dib-Hajj et al., 2015). Given its inhibitory effects on $\text{Nav}_{1.8/1.9}$, HSTX-I likely exerts analgesic functions. As illustrated in **Figure 3A**, HSTX-I reduced the response of pain in both the first (neurogenic pain, 0–5 min) and the second phases (inflammatory pain, 15–30 min) in formalin-induced paw licking mouse model, suggesting that HSTX-I has similar effect on both neurogenic and inflammatory pain. In the first

phase, licking time was reduced 25.4% ($P < 0.01$) and 36.5% ($P < 0.01$) by 1.25 and 2.5 $\mu\text{mol/kg}$ HSTX-I, while in the second phase, the licking time was reduced 9.8 and 24.6% ($P < 0.01$), respectively. In the mouse model of abdominal writhing induced by acetic acid, 1.25 and 2.5 $\mu\text{mol/kg}$ HSTX-I decreased writhing time by 15.5 and 28.8% ($P < 0.01$), respectively (**Figure 3B**). Hot plate model of mouse showed that the latency of pain response was delayed by intraperitoneal administration of HSTX-I. The latency was delayed 10.7 and 29% ($P < 0.05$) by 1.25 and 2.5 $\mu\text{mol/kg}$ HSTX-I, respectively (**Figure 3C**). HSTX-I showed outstanding analgesic functions in several mouse models.

DISCUSSION

Voltage-gated sodium channels are integral transmembrane proteins that play a key role for the rapid depolarization of excitable cells (Hodgkin and Huxley, 1952). Their importance to pain perception is indisputable (Bagal et al., 2014). Activation of TTX-R sodium channels, especially $\text{Nav}_{1.8}$, contributes to action potential electrogenesis in neurons (Akopian et al., 1996; Jarvis et al., 2007). $\text{Nav}_{1.8}$ carries the majority of the current underlying the upstroke of the action potential in nociceptive neurons (Akopian et al., 1999; Renganathan et al., 2001). Recent genetic and functional findings indicate that $\text{Nav}_{1.9}$ is linked to human pain disorder (Dennison et al., 2015). In order to successfully

get blood meals and to anesthetize hosts, leeches possibly utilize salivary compounds acting on TTX-R sodium channels to inhibit activation of nociceptive neurons and overcome pain. Clinical experiments strongly indicate that leech therapy produces a strong and long lasting pain-reducing effect although no specific analgesic substance has been found.

The small peptide HSTX-I (ACKEYWECGAFLEFCIEGI CVPMI), which contains high density of half-cysteines as neurotoxins acting on ion channels, was identified and characterized from the leech salivary glands of *H. sylvestrus* (Figure 1). It inhibited TTX-R Na⁺ channel currents and had no effect on voltage-gated Ca²⁺, K⁺, and TTX-S Na⁺ currents (Supplementary Figure 3). HSTX-I reduced Nav1.8/1.9 currents but only shifted steady-state activation of Nav1.9 to hyperpolarization (Figure 2F). This finding indicated the effects of HSTX-I on Nav1.8 and Nav1.9 were slightly different. HSTX-I may interact with different domains of Nav1.8 and Nav1.9. Further mutations experiments may give an answer. Due to its selective activity on Nav1.8 and Nav1.9, HSTX-I could be a valuable tool for the study of Nav1.8 and Nav1.9.

It is noted that Nav1.8 is cold resistant, meaning that it is essential for pain and in maintaining the excitability of nociceptors at low temperatures (Renganathan et al., 2001). HSTX-I possibly blocks excitability of host nociceptors at low temperatures, such as water environment where leeches' generally inhabit. HSTX-I showed outstanding analgesic activity in several mouse models (Figure 3). It reduced the response of pain at both first (neurogenic pain, 0–5 min) and second phase (inflammatory pain, 15–30 min) with similar efficiency, suggesting that HSTX-I has similar effect on both neurogenic and inflammatory pain (Figure 3A). Nav1.8/1.9 may be safe targets for treatment of chronic pain because knocking out Nav1.8 or Nav1.9 in mice showed little adverse effects. HSTX-I selectively acted on Nav1.8/1.9 and showed significant analgesic effects in animal models, indicating it may be a promising lead molecule for development of analgesics.

CONCLUSION

A novel peptide HSTX-I from *H. sylvestrus* inhibited sodium channels (Nav1.8 and Nav1.9) and exerted direct analgesic

REFERENCES

- Akopian, A. N., Sivilotti, L., and Wood, J. N. (1996). A tetrodotoxin-resistant voltage-gated sodium channel expressed by sensory neurons. *Nature* 379, 257–262. doi: 10.1038/379257a0
- Akopian, A. N., Souslova, V., England, S., Okuse, K., Ogata, N., Ure, J., et al. (1999). The tetrodotoxin-resistant sodium channel SNS has a specialized function in pain pathways. *Nat. Neurosci.* 2, 541–548. doi: 10.1038/9195
- An, S., Chen, L., Long, C., Liu, X., Xu, X., Lu, X., et al. (2013). Dermatophagoides farinae allergens diversity identification by proteomics. *Mol. Cell. Proteomics* 12, 1818–1828. doi: 10.1074/mcp.M112.027136
- Bagal, S. K., Chapman, M. L., Marron, B. E., Prime, R., Storer, R. I., and Swain, N. A. (2014). Recent progress in sodium channel modulators for pain. *Bioorg. Med. Chem. Lett.* 24, 3690–3699. doi: 10.1016/j.bmcl.2014.06.038

function. The discovery of analgesic peptide HSTX-I in the leech enriches our understanding of the molecular mechanisms of feeding strategies for hematophagous leeches. In addition, the current work is historically relevant because it reveals the specific analgesic substance and their pharmacological mechanisms in leech therapies.

AUTHOR CONTRIBUTIONS

RL, ZS, and XL designed the study and wrote the paper. GW and CL conducted most of the experiments, analyzed the results, and wrote the paper. WL and MZ conducted experiments on the purification of peptides. QL and PM conducted experiments on screening for ion channel function. CX and DL evaluated analgesic activity *in vivo*. QML and MR provided technical assistance and contributed to the preparation of the figures. All authors analyzed the results and approved the final version of the manuscript.

FUNDING

This work was supported by funding from National Natural Science Foundation of China (31630075, 31600721, and 21761142002), Chinese Academy of Sciences (SAJC201606, 2015CASEABRI002, and ZSTH-017), and Yunnan Province (2016FA006 and 2015BC005).

ACKNOWLEDGMENTS

We thank our lab member Dr. Shilong Yang for assistance and discussion.

SUPPLEMENTARY MATERIAL

The Supplementary Material for this article can be found online at: <https://www.frontiersin.org/articles/10.3389/fphar.2018.00186/full#supplementary-material>

- Baker, M. D. (2005). Protein kinase C mediates up-regulation of tetrodotoxin-resistant, persistent Na⁺ current in rat and mouse sensory neurones. *J. Physiol.* 567, 851–867. doi: 10.1113/jphysiol.2005.08.9771
- Baker, M. D., Chandra, S. Y., Ding, Y., Waxman, S. G., and Wood, J. N. (2003). GTP-induced tetrodotoxin-resistant Na⁺ current regulates excitability in mouse and rat small diameter sensory neurones. *J. Physiol.* 548, 373–382. doi: 10.1113/jphysiol.2003.039131
- Benn, S. C., Costigan, M., Tate, S., Fitzgerald, M., and Woolf, C. J. (2001). Developmental expression of the TTX-resistant voltage-gated sodium channels Nav1.8 (SNS) and Nav1.9 (SNS2) in primary sensory neurons. *J. Neurosci.* 21, 6077–6085.
- Blum, R., Kafitz, K. W., and Konnerth, A. (2002). Neurotrophin-evoked depolarization requires the sodium channel Na(V)1.9. *Nature* 419, 687–693. doi: 10.1038/nature01085

- Cummins, T. R., Dib-Hajj, S. D., Black, J. A., Akopian, A. N., Wood, J. N., and Waxman, S. G. (1999). A novel persistent tetrodotoxin-resistant sodium current in SNS-null and wild-type small primary sensory neurons. *J. Neurosci.* 19:RC43.
- Dennison, S. R., Mura, M., Harris, F., Morton, L. H., Zvelindovsky, A., and Phoenix, D. A. (2015). The role of C-terminal amidation in the membrane interactions of the anionic antimicrobial peptide, maximin H5. *Biochim. Biophys. Acta* 1848, 1111–1118. doi: 10.1016/j.bbame.2015.01.014
- Dib-Hajj, S., Black, J. A., Cummins, T. R., and Waxman, S. G. (2002). NaN/Nav1.9: a sodium channel with unique properties. *Trends Neurosci.* 25, 253–259. doi: 10.1016/S0166-2236(02)02150-1
- Dib-Hajj, S. D., Black, J. A., and Waxman, S. G. (2015). Nav1.9: a sodium channel linked to human pain. *Nat. Rev. Neurosci.* 16, 511–519. doi: 10.1038/nrn3977
- Dib-Hajj, S. D., Tyrrell, L., Black, J. A., and Waxman, S. G. (1998). NaN, a novel voltage-gated Na channel, is expressed preferentially in peripheral sensory neurons and down-regulated after axotomy. *Proc. Natl. Acad. Sci. U.S.A.* 95, 8963–8968. doi: 10.1073/pnas.95.15.8963
- Faber, C. G., Lauria, G., Merkies, I. S., Cheng, X., Han, C., Ahn, H. S., et al. (2012). Gain-of-function Nav1.8 mutations in painful neuropathy. *Proc. Natl. Acad. Sci. U.S.A.* 109, 19444–19449. doi: 10.1073/pnas.1216080109
- Fang, X., Djouhri, L., Black, J. A., Dib-Hajj, S. D., Waxman, S. G., and Lawson, S. N. (2002). The presence and role of the tetrodotoxin-resistant sodium channel Na(v)1.9 (NaN) in nociceptive primary afferent neurons. *J. Neurosci.* 22, 7425–7433.
- Han, C., Vasylyev, D., Macala, L. J., Gerrits, M. M., Hoeijmakers, J. G., Bekelaar, K. J., et al. (2014). The G1662S Nav1.8 mutation in small fibre neuropathy: impaired inactivation underlying Drg neuron hyperexcitability. *J. Neurol. Neurosurg. Psychiatry* 85, 499–505. doi: 10.1136/jnnp-2013-306095
- Hodgkin, A. L., and Huxley, A. F. (1952). A quantitative description of membrane current and its application to conduction and excitation in nerve. *J. Physiol.* 117, 500–544. doi: 10.1113/jphysiol.1952.sp004764
- Hosseini, S., Naderi-Manesh, H., Mountassif, D., Cerruti, M., Vali, H., and Faghihi, S. (2013). C-terminal amidation of an osteocalcin-derived peptide promotes hydroxyapatite crystallization. *J. Biol. Chem.* 288, 7885–7893. doi: 10.1074/jbc.M112.422048
- Huang, J., Han, C., Estacion, M., Vasylyev, D., Hoeijmakers, J. G., Gerrits, M. M., et al. (2014). Gain-of-function mutations in sodium channel Na(v)1.9 in painful neuropathy. *Brain* 137, 1627–1642. doi: 10.1093/brain/awu079
- Huang, J., Vanoye, C. G., Cutts, A., Goldberg, Y. P., Dib-Hajj, S. D., Cohen, C. J., et al. (2017). Sodium channel Nav1.9 mutations associated with insensitivity to pain dampen neuronal excitability. *J. Clin. Invest.* 127, 2805–2814. doi: 10.1172/JCI92373
- Huang, J., Yang, Y., Zhao, P., Gerrits, M. M., Hoeijmakers, J. G., Bekelaar, K., et al. (2013). Small-fiber neuropathy Nav1.8 mutation shifts activation to hyperpolarized potentials and increases excitability of dorsal root ganglion neurons. *J. Neurosci.* 33, 14087–14097. doi: 10.1523/JNEUROSCI.2710-13.2013
- Hyson, J. M. (2005). Leech therapy: a history. *J. Hist. Dent.* 53, 25–27.
- Intlekofer, K. A., Berchtold, N. C., Malvaez, M., Carlos, A. J., McQuown, S. C., Cunningham, M. J., et al. (2013). Exercise and sodium butyrate transform a subthreshold learning event into long-term memory via a brain-derived neurotrophic factor-dependent mechanism. *Neuropsychopharmacology* 38, 2027–2034. doi: 10.1038/npp.2013.104
- Jarvis, M. F., Honore, P., Shieh, C. C., Chapman, M., Joshi, S., Zhang, X. F., et al. (2007). A-803467, a potent and selective Nav1.8 sodium channel blocker, attenuates neuropathic and inflammatory pain in the rat. *Proc. Natl. Acad. Sci. U.S.A.* 104, 8520–8525. doi: 10.1073/pnas.0611364104
- Koeppen, D., Aurich, M., and Rampp, T. (2014). Medicinal leech therapy in pain syndromes: a narrative review. *Wien. Med. Wochenschr.* 164, 95–102. doi: 10.1007/s10354-013-0236-y
- Leipold, E., Hanson-Kahn, A., Frick, M., Gong, P., Bernstein, J. A., Voigt, M., et al. (2015). Cold-aggravated pain in humans caused by a hyperactive Nav1.9 channel mutant. *Nat. Commun.* 6:10049. doi: 10.1038/ncomms10049
- Leipold, E., Liebmann, L., Korenke, G. C., Heinrich, T., Giesselmann, S., Baets, J., et al. (2013). A de novo gain-of-function mutation in SCN11A causes loss of pain perception. *Nat. Genet.* 45, 1399–1404. doi: 10.1038/ng.2767
- Lolignier, S., Bonnet, C., Gaudio, C., Noel, J., Ruel, J., Amsalem, M., et al. (2015). The Nav1.9 channel is a key determinant of cold pain sensation and cold allodynia. *Cell Rep.* 11, 1067–1078. doi: 10.1016/j.celrep.2015.04.027
- O'Brien, B. J., Caldwell, J. H., Ehring, G. R., Bumsted O'brien, K. M., Luo, S., and Levinson, S. R. (2008). Tetrodotoxin-resistant voltage-gated sodium channels Na(v)1.8 and Na(v)1.9 are expressed in the retina. *J. Comp. Neurol.* 508, 940–951. doi: 10.1002/cne.21701
- Ostman, J. A., Nassar, M. A., Wood, J. N., and Baker, M. D. (2008). Gtp up-regulated persistent Na⁺ current and enhanced nociceptor excitability require Nav1.9. *J. Physiol.* 586, 1077–1087. doi: 10.1113/jphysiol.2007.147942
- Padilla, F., Couble, M. L., Coste, B., Maingret, F., Clerc, N., Crest, M., et al. (2007). Expression and localization of the Nav1.9 sodium channel in enteric neurons and in trigeminal sensory endings: implication for intestinal reflex function and orofacial pain. *Mol. Cell. Neurosci.* 35, 138–152. doi: 10.1016/j.mcn.2007.02.008
- Rados, C. (2004). Beyond bloodletting: FDA gives leeches a medical makeover. *FDA Consum.* 38:9.
- Renganathan, M., Cummins, T. R., and Waxman, S. G. (2001). Contribution of Na(v)1.8 sodium channels to action potential electrogenesis in DRG neurons. *J. Neurophysiol.* 86, 629–640. doi: 10.1152/jn.2001.86.2.629
- Ritter, A. M., Martin, W. J., and Thorneloe, K. S. (2009). The voltage-gated sodium channel Nav1.9 is required for inflammation-based urinary bladder dysfunction. *Neurosci. Lett.* 452, 28–32. doi: 10.1016/j.neulet.2008.12.051
- Rugiero, F., Mistry, M., Sage, D., Black, J. A., Waxman, S. G., Crest, M., et al. (2003). Selective expression of a persistent tetrodotoxin-resistant Na⁺ current and Nav1.9 subunit in myenteric sensory neurons. *J. Neurosci.* 23, 2715–2725.
- Rush, A. M., and Waxman, S. G. (2004). PGE2 increases the tetrodotoxin-resistant Nav1.9 sodium current in mouse Drg neurons via G-proteins. *Brain Res.* 1023, 264–271. doi: 10.1016/j.brainres.2004.07.042
- Shields, S. D., Ahn, H. S., Yang, Y., Han, C., Seal, R. P., Wood, J. N., et al. (2012). Nav1.8 expression is not restricted to nociceptors in mouse peripheral nervous system. *Pain* 153, 2017–2030. doi: 10.1016/j.pain.2012.04.022
- Singh, A. P. (2010). Medicinal leech therapy (hirudotherapy): a brief overview. *Complement. Ther. Clin. Pract.* 16, 213–215. doi: 10.1016/j.ctcp.2009.11.005
- Swanwick, R. S., Pristera, A., and Okuse, K. (2010). The trafficking of Na(V)1.8. *Neurosci. Lett.* 486, 78–83. doi: 10.1016/j.neulet.2010.08.074
- Waxman, S. G., Cummins, T. R., Dib-Hajj, S., Fjell, J., and Black, J. A. (1999). Sodium channels, excitability of primary sensory neurons, and the molecular basis of pain. *Muscle Nerve* 22, 1177–1187. doi: 10.1002/(SICI)1097-4598(199909)22:9<1177::AID-MUS3>3.0.CO;2-P
- Wu, J., Gage, D. A., and Watson, J. T. (1996). A strategy to locate cysteine residues in proteins by specific chemical cleavage followed by matrix-assisted laser desorption ionization time-of-flight mass spectrometry. *Anal. Biochem.* 235, 161–174. doi: 10.1006/abio.1996.0108
- Xu, M., Gruber, B. D., Delhaize, E., White, R. G., James, R. A., You, J., et al. (2015). The barley anion channel, HvALMT1, has multiple roles in guard cell physiology and grain metabolism. *Physiol. Plant.* 153, 183–193. doi: 10.1111/ppl.12234
- Yam, M. F., Asmawi, M. Z., and Basir, R. (2008). An investigation of the anti-inflammatory and analgesic effects of *Orthosiphon stamineus* leaf extract. *J. Med. Food* 11, 362–368. doi: 10.1089/jmf.2006.065
- Yang, S., Xiao, Y., Kang, D., Liu, J., Li, Y., Undheim, E. A., et al. (2013). Discovery of a selective Nav1.7 inhibitor from centipede venom with analgesic efficacy exceeding morphine in rodent pain models. *Proc. Natl. Acad. Sci. U.S.A.* 110, 17534–17539. doi: 10.1073/pnas.1306285110
- Zhang, X. Y., Wen, J., Yang, W., Wang, C., Gao, L., Zheng, L. H., et al. (2013). Gain-of-function mutations in SCN11A cause familial episodic pain. *Am. J. Hum. Genet.* 93, 957–966. doi: 10.1016/j.ajhg.2013.09.016
- Zimmermann, K., Leffler, A., Babes, A., Cendan, C. M., Carr, R. W., Kobayashi, J., et al. (2007). Sensory neuron sodium channel Nav1.8 is essential for pain at low temperatures. *Nature* 447, 855–858. doi: 10.1038/nature05880

Conflict of Interest Statement: The authors declare that the research was conducted in the absence of any commercial or financial relationships that could be construed as a potential conflict of interest.

Copyright © 2018 Wang, Long, Liu, Xu, Zhang, Li, Lu, Meng, Li, Rong, Sun, Luo and Lai. This is an open-access article distributed under the terms of the Creative Commons Attribution License (CC BY). The use, distribution or reproduction in other forums is permitted, provided the original author(s) and the copyright owner are credited and that the original publication in this journal is cited, in accordance with accepted academic practice. No use, distribution or reproduction is permitted which does not comply with these terms.